

(CD₂Cl₂) δ 11.77 (br d, J = 11.5 Hz, μ -CH), 5.48, 5.21 (10 H, C₅H₅), 3.38 (dd, J = 11.5, 10 Hz, =CH), 1.90 (dq, J = 10, 6.7 Hz, CHMe), 1.14 (s, 9 H, CH₃), 1.04 (d, J = 6.7 Hz, 3 H, CH₃); ¹³C{¹H} NMR (CD₃NO₂) δ 241.4 (μ -CO), 215.1 (CO), 174.6 (μ -CH), 108.2 (=CHR), 92.7, 89.8 (C₅H₅), 54.9 (CH=CHC), 36.1 (CMe₃), 28.3 (C(CH₃)₃), 16.7 (CH₃); IR (CH₂Cl₂) 2020 (s), 1995 (w), 1864 (m) cm⁻¹. Anal. Calcd for C₂₁H₂₅F₆Fe₂O₃P: C, 43.33; H, 4.33. Found: C, 43.20; H, 4.22.

Similarly, reaction of 2,3,3-trimethyl-1-butene (21 mg, 0.21 mmol) with **1-d** (60 mg, 0.12 mmol) in CH₂Cl₂ gave **7-d** (55 mg, 76%): ²H{¹H} NMR (acetone) δ 12.15.

[(C₅H₅)₂(CO)Fe]₂(μ -CO)[μ -CHCH=C(CH₃)(C(CH₃)₃)] (**8**). 2,3,3-Trimethyl-1-butene (100 μ L, 0.72 mmol) was added to a stirred suspension of **1** (102 mg, 0.21 mmol) in CH₂Cl₂ (50 mL) at -78 °C. The reaction mixture was stirred at ambient temperature for 35 min and then cooled to -50 °C. Trimethylamine (0.92 atm, 235 mL, 8.9 mmol) was added, and solvent was evaporated at ambient temperature. The resulting solid was purified by column chromatography (alumina, 4:1 hexane/CH₂Cl₂) to give **8** (74 mg, 81%): ¹H NMR (acetone-*d*₆) δ 12.31 (d, J = 13 Hz, μ -CH), 6.80 (d, J = 13.0 Hz, =CH), 4.86 (s, C₅H₅), 2.14 (s, CH₃), 1.09 (s, C(CH₃)₃); ¹³C NMR (CD₂Cl₂) δ 274.5 (μ -CO), 213.2 (CO), 161.8 (d, J = 133 Hz, μ -CHR), 150.0 (d, J = 154 Hz, CH=CR₂), 131.7 (CH=CR₂), 87.1 (d, J = 178 Hz, C₅H₅), 36.3 (CMe₃), 28.9 (q, J = 126 Hz, C(CH₃)₃), 13.3 (q, J = 127 Hz, CH₃); IR (CH₂Cl₂) 1978 (s), 1940 (m), 1777 (m) cm⁻¹; HRMS calcd for C₂₁H₂₄Fe₂O₃ 436.0417, found 436.0419.

Similarly, a solution of 2,3,3-trimethyl-1-butene (100 μ L, 0.72 mmol) and **1-d** (90 mg, 0.186 mmol) was reacted with NMe₃ (1.0 atm, 235 mL, 10 mmol) to give **8-d** (73 mg, 90%): ²H{¹H} NMR (acetone) δ 12.3.

[(C₅H₅)₂(CO)Fe]₂(μ -CO)[μ -CHCH=C(C₆H₅)₂] (**9**). 1,1-Diphenylethylene (95 μ L, 97 mg, 0.54 mmol) was added to a stirred solution of **1** (160 mg, 0.331 mmol) in CH₂Cl₂ (40 mL) at -30 °C. A saturated aqueous solution of NaHCO₃ (3 mL) and acetone (10 mL) was added at ambient temperature. The solution was dried (MgSO₄), filtered, and evaporated to dryness. The resulting solid was purified by column chromatography (alumina, CH₂Cl₂) and crystallization from CH₂Cl₂-hexane solution to give **9** (80 mg, 46%) as dark red crystals: ¹H NMR (acetone-*d*₆) δ 11.37 (d, J = 13.4 Hz, μ -CH), 7.7-7.1 (m, 11 H, C₆H₅ and μ -CH=CHR), 4.76 (s, 10 H, C₅H₅); ¹³C{¹H} NMR (acetone-*d*₆) δ

271.5 (μ -CO), 214.6 (CO), 157.8 (μ -CHR), 143.6, 142.8, 131.5, 129.4, 127.9, 127.1 (C₆H₅ and C=C), 88.7 (C₅H₅); IR (CH₂Cl₂) 1976 (s), 1941 (m), 1782 (m) cm⁻¹; HRMS calcd for C₂₈H₂₂Fe₂O₃ 518.0261, found 518.0263.

[(C₅H₅)₂(CO)Fe]₂(μ -CO)[μ -CHCH=C(CH₃)(C₆H₅)] (**10-E** and **10-Z**). A saturated aqueous solution of NaHCO₃ (1.5 mL) was added to a stirred solution of **6** (45 mg, 0.075 mmol) in acetone (10 mL). Solvent was evaporated, and the resulting solid was purified by column chromatography (alumina, Et₂O) to give a 70:30 mixture of **10-E** and **10-Z** (15 mg, 44%): ¹H NMR (acetone-*d*₆) major isomer, **10-E**, δ 12.18 (d, J = 13.4 Hz, μ -CHR), 7.6-7.2 (m, C₆H₅ and =CHR), 4.95 (s, C₅H₅), 2.50 (s, CH₃); minor isomer, **10-Z**, δ 11.58 (d, J = 13 Hz, μ -CH), 7.6-7.2 (m, C₆H₅), 6.86 (d, J = 13.4 Hz, =CH), 4.70 (s, C₅H₅), 2.09 (s, CH₃); ¹³C NMR (acetone-*d*₆) major isomer, **10-E** δ 272.3 (μ -CO), 214.5 (CO), 160.1 (d, J = 137 Hz, μ -CHR), 157.1 (d, J = 155 Hz, =CHR), 145.0 (ipso, C₆H₅), 129.3 (d, J = 157 Hz, C₆H₅), 126.5 (d, J = 155 Hz, C₆H₅), 126.0 (=CMePh), 88.6 (d, J = 175 Hz, C₅H₅), 25.9 (q, J = 121 Hz, CH₃); minor isomer, **10-Z**, δ 157.6 (d, J = 130 Hz, μ -CHR), 155.4 (d, J = 154 Hz, =CHR), 122.0 (=CMePh), 16.2 (q, J = 128 Hz, CH₃); IR (CH₂Cl₂) 1975 (s), 1945 (w), 1777 (m) cm⁻¹; HRMS calcd for C₂₃H₂₀Fe₂O₃ 456.0105, found 456.0105.

Similarly, treatment of **6-d** (60 mg, 0.10 mmol) with NaHCO₃ gave a 70:30 mixture of **10-E-d** and **10-Z-d** (20 mg, 44%): ²H{¹H} NMR (CH₂Cl₂) δ 12.1, 11.6.

Acknowledgment. Support from the National Science Foundation is gratefully acknowledged.

Registry No. **1**, 82660-14-8; **1-d**, 90388-70-8; **2**, 102234-50-4; **2-d**, 102260-79-7; **3**, 102234-52-6; **4**, 102234-54-8; **4-d**, 102234-65-1; **5**, 102234-56-0; **6**, 102234-58-2; **6-d**, 102234-67-3; **7**, 102234-60-6; **7-d**, 102234-69-5; **8-E**, 102234-61-7; **8-E-d**, 102234-70-8; **8-Z**, 102339-55-9; **8-Z-d**, 102339-56-0; **9**, 102234-62-8; **10-E**, 102234-63-9; **10-E-d**, 102234-71-9; **10-Z**, 102339-53-7; **10-Z-d**, 102339-54-8; 1-methylcyclohexene, 591-49-1; (2-methyl-1-propenyl)benzene, 768-49-0; *trans*-stilbene, 103-30-0; 1,1-diphenylethylene, 530-48-3; 1,1-di-*p*-tolylethylene, 2919-20-2; α -methylstyrene, 98-83-9; 2,3,3-trimethyl-1-butene, 7439-89-6; Fe, 7439-89-6; D₂, 7782-39-0.

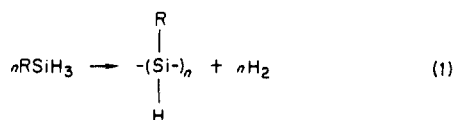
Identification of Some Intermediates in the Titanocene-Catalyzed Dehydrogenative Coupling of Primary Organosilanes

Clare T. Aitken,^{1a} John F. Harrod,^{*1a} and Edmond Samuel^{1b}

Contribution from the Department of Chemistry, McGill University, Montreal, Canada H3A 2K6, and Laboratoire de Chimie Organique Industrielle, UA 403, CNRS, ENSCP, Paris, 75231 CEDEX 05, France. Received December 20, 1985

Abstract: Two new compounds, **2** and **3**, were observed by NMR spectroscopy in PhSiH₃ undergoing dehydrogenative polymerization under the catalytic influence of Cp₂Ti(CH₃)₂. With use of slightly different reaction conditions, these two compounds were synthesized in good yields and their structures established by NMR spectroscopy and X-ray crystallography. Compound **2** is a dimer of Cp₂TiSiH₂Ph in which dimerization occurs through a pair of Ti-H-Si bridges. Compound **3** has the structure [Cp₂Ti(μ -H)(μ -HSiHPh)TiCp₂]. Under ambient conditions **2** spontaneously decomposes into **3** with production of poly(phenylsilane). **3** is transformed into **2** in the presence of excess PhSiH₃. Some chemistry and ESR spectroscopic properties of these two unusual compounds are described, and their possible involvement in the polymerization reaction is discussed.

We have recently reported the dehydrogenative coupling of primary organosilanes to linear polysilanes, under the catalytic influence of dialkyltitanocenes and zirconocenes^{2,3} (eq 1). This



(1) (a) McGill University. (b) Ecole Nationale Supérieure de Chimie de Paris.

reaction provides a facile new method for the generation of Si-Si bonds which gives no obnoxious byproducts and furnishes polysilanes of a type not easily accessible by the classical routes of active metal dehalogenation of halosilanes.⁴

(2) Aitken, C.; Harrod, J. F.; Samuel, E. *J. Organomet. Chem.* **1985**, 279, C11.

(3) Harrod, J. F.; Aitken, C. International Chemical Congress of the Pacific Basin Society, Honolulu, Dec 16-21, 1984, Paper 7K12.

(4) For an excellent review of the chemistry of polysilanes see: West, R. *Comprehensive Organometallic Chemistry*; Pergamon Press: New York, 1982; Vol. 2, Chapter 9, p 365.

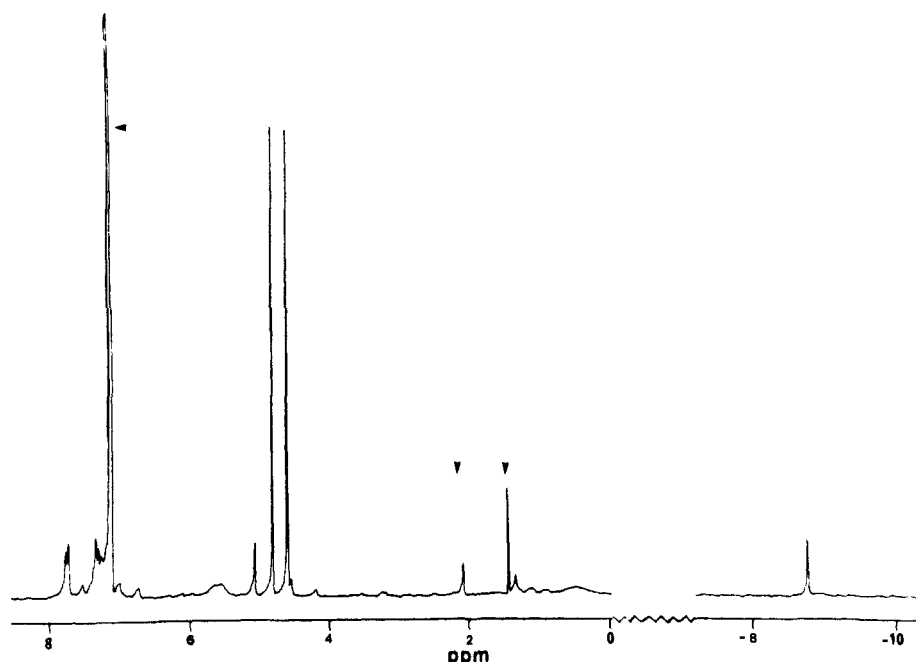
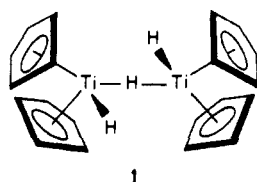


Figure 1. 200-MHz ^1H NMR spectrum of **2** in C_6D_6 at 20°C . An arrowhead denotes peaks due to impurities.

Because the polymerization reaction (eq 1) appears to yield no cyclic or short linear oligomers, it seems most likely that the polymerization proceeds by repetitive insertion of a silene moiety into a metal–Si bond. We therefore undertook to detect and if possible to isolate the titanocene intermediates involved in the reaction of dimethyltitanocene with phenylsilane.

From earlier studies using ESR spectroscopy, we had established the presence of a paramagnetic, mixed valence, titanocene hydride derivative, **1**, as a product of the reactions of dialkyltitanocenes with a number of primary, secondary, and tertiary silicon hydrides.⁵ For the phenylsilane reaction we have now isolated and structurally characterized two new complexes of unusual structure, both of which seems to be actively involved in the catalytic cycle of eq 1.

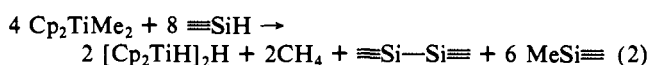


Results

Some General Observations Concerning the Reactions of Silicon Hydrides with Dimethyltitanocene. A number of titanocene derivatives, Cp_2TiR_2 ($\text{Cp}_2 =$ bis(cyclopentadienyl), cyclopentadienylmethylcyclopentadienyl, bis(methylcyclopentadienyl), and bis(indenyl), but not cyclopentadienylpentamethylcyclopentadienyl or bis(pentamethylcyclopentadienyl); $\text{R} =$ methyl or benzyl, but not phenyl), have been found to undergo a similar reaction with a variety of silicon hydrides (RSiH_3 , where $\text{R} =$ phenyl, benzyl, or *n*-hexyl; R_2SiH_2 , where $\text{R}_2 =$ diphenyl, phenylmethyl, or methylbutyl; $[\text{RO}]_3\text{SiH}$, where $\text{R} =$ methyl or ethyl, $[\text{EtO}]_2\text{MeSiH}$, and 1,3,5,7-tetramethylcyclotetrasiloxane). Chlorosilanes give a different reaction and tertiary alkyl- or arylsilanes do not react at all. This reaction is characterized by the following features. After the reagents are mixed in an aliphatic or aromatic solvent, there is an induction period during which no observable change takes place in the orange solution. This induction period varies from a few seconds to a few hours, depending on the composition of the silane and the concentrations of the

reactants. The end of the induction period is signalled by the appearance of a few gas bubbles, followed by an accelerating gas evolution. The gas was shown by IR and MS to be methane, or a mixture of hydrogen and methane, depending on the silane. Shortly after the appearance of gas, dark blue wisps appear which grow and spread through the medium, partly as a result of the turbulence created by the gas evolution, until the whole solution becomes uniformly inky blue. On standing, crystalline products deposit from solution. The product is usually a mixture of compounds, and the present paper concerns itself with the separation and isolation of some of the compounds produced when the reactants are dimethyltitanocene and phenylsilane. For all of the silanes listed above compound **1** is observed as one of the main products, identified by its highly characteristic signal in the ESR.⁵

In a preliminary communication we proposed the stoichiometry of eq 2 for the production of **1** by reaction of silicon hydrides with



dimethyltitanocene. It is now clear that this equation is an oversimplification and that a number of other reactions occur, producing other titanium-containing products. However, it is still true that **1** is always an important product and in many cases the major product. The methylsilane product has been observed for the reactions of PhSiH_3 and Ph_2SiH_2 . The production of disilane has been verified for the Ph_2SiH_2 reaction.

When the reaction is carried out under an atmosphere of CO, the appearance of the blue products is suppressed and there is instead a slow accumulation of titanocene dicarbonyl in the solution. Purging of the CO with an inert gas results in immediate and rapid production of the blue products.

^1H NMR Studies. In the presence of catalytic amounts of dimethyltitanocene, the ^1H NMR spectrum of an actively polymerizing PhSiH_3 reaction in C_6D_6 reveals, in addition to the resonances of the monomer and polymer, the presence of a titanocene species with two inequivalent Cp groups (δ 4.65 and 4.86), a single Si–H resonance (δ 5.11) and a single hydride resonance at high field (δ –8.73). This assignment was confirmed by the fact that only the Cp resonances were evident when PhSiD_3 was used as reactant to eliminate the interfering SiH resonances in the Cp region. Compound **2** was subsequently prepared in high yield by reaction of dimethyltitanocene with moderate molar excesses of PhSiH_3 (ca. 3:1) in a variety of hydrocarbon and ether solvents. The purified compound gave the ^1H NMR spectrum shown in Figure 1. Integration of this spectrum reveals that **2**

(5) Samuel, E.; Harrod, J. F. *J. Am. Chem. Soc.* **1984**, *106*, 1859.

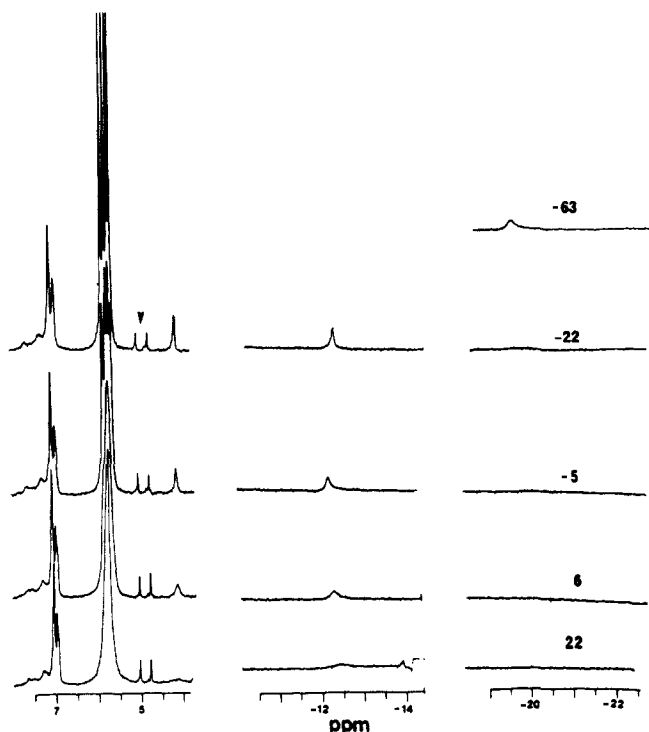


Figure 2. 200-MHz ^1H NMR spectrum of **3** in THF. The numbers at the right denote the probe temperature in $^{\circ}\text{C}$. An arrowhead denotes the Cp resonances of a trace of **2**.

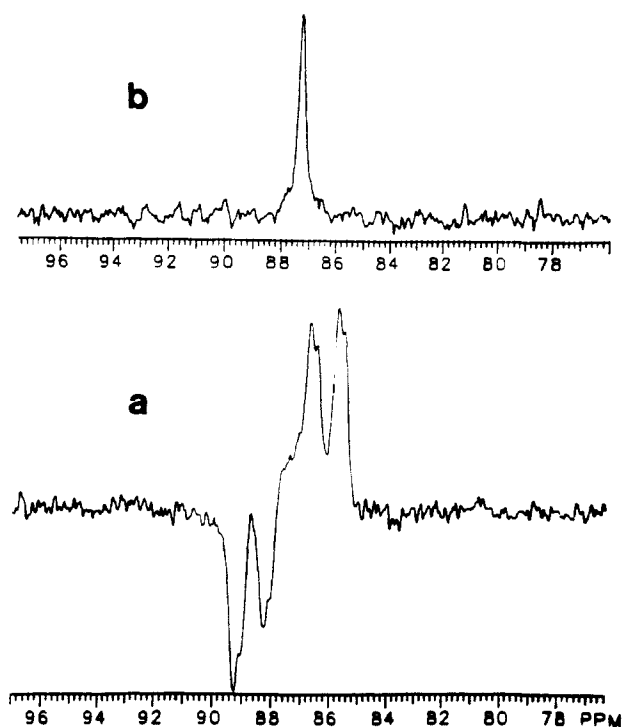


Figure 3. ^{29}Si NMR spectrum of **3** with use of an INEPT¹⁴ pulse sequence at 59.59 MHz: (a) proton coupled, (b) proton decoupled.

contains the elements of $[\text{Cp}_2\text{Ti}(\text{H})\text{SiHPh}]$. The Cp groups are inequivalent, and in addition there is one conventional Si-H resonance and a single hydride at high field. The spectrum is readily assigned to the structure shown in Figure 4 if it assumed that the high-field resonance is due to the Ti-H-Si proton. Similar reactions with *n*-hexyl- and benzylsilane gave similar results except that the Cp and hydride resonances were doubled, indicating the presence of a major and a minor isomer. Pure compounds were not successfully isolated from these reactions.

Compound **2** is unstable in solution and decomposes to a new compound, **3**, and polysilane under ambient conditions. The

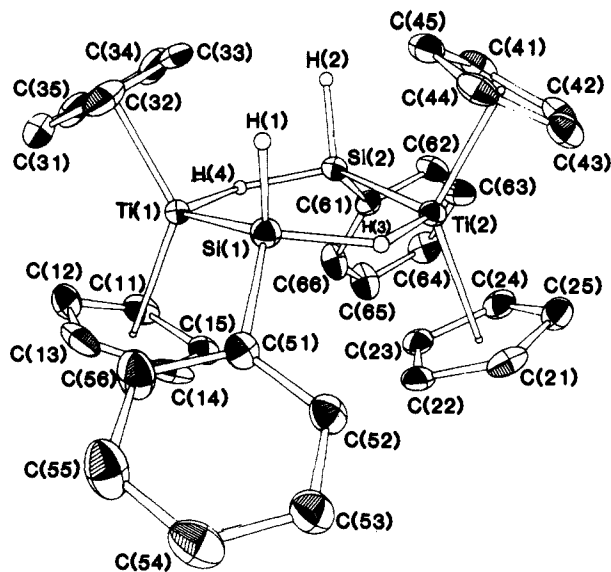


Figure 4. An Ortep drawing of a single molecule of **2** showing the numbering scheme used in Tables III, VII, IX, and XI. Hydrogen atoms on the ligand rings are omitted for the sake of clarity.

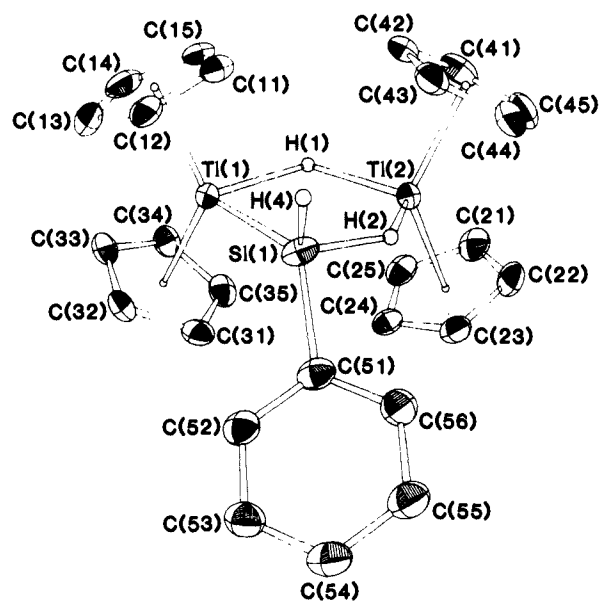


Figure 5. An Ortep drawing of a single molecule of **3** showing the numbering scheme used in Tables VII, VIII, X, and XII. Hydrogen atoms are omitted for the sake of clarity.

presence of **3** is apparent from a broad resonance at room temperature in the Cp region (see Figure 1, δ 5.62) which is evident even in solutions of freshly prepared **2** and which was initially attributed to the presence of paramagnetic impurities. However, on lowering the temperature the broad signal splits into four sharp resonances at ca. -10 to -20 $^{\circ}\text{C}$, depending on solvent, and a high-field hydride resonance appears at ca. -12 ppm. On further lowering the temperature a second high-field hydride resonance appears at ca. -20 ppm. Compound **3** was synthesized in a relatively pure state from a reaction of dimethyltitanocene and PhSiH_3 in a 1:1 molar ratio in diethyl ether. The NMR spectrum of **3** at several temperatures in tetrahydrofuran- d_8 is shown in Figure 2. Integration of this spectrum indicates the formula $[\text{Cp}_2\text{Ti}(\text{H})(\text{SiHPh})(\text{H}')\text{TiCp}_2]$ for the compound, where (H) and (H') are the two inequivalent, high-field protons. A ^{29}Si NMR spectrum (Figure 3) revealed coupling of the Si to two inequivalent geminal protons (148 and 58 Hz) and a weak coupling to a third proton (14 Hz). The very low symmetry of the molecule, together with the striking similarity of the hydride region of the NMR spectrum to that of the previously reported compound $[\text{CpTi}(\mu\text{-H})(\mu\text{-AlH}_2\text{Et}_2)(\mu\text{-C}_{10}\text{H}_8)\text{TiCp}]$,⁶ allowed assignment of the

Table I. Crystal Data and Parameters for Data Collection for $[\text{Cp}_2\text{TiSiH}_2\text{Ph}]_2$ (**2**)

formula	$\text{C}_{32}\text{H}_{34}\text{Si}_2\text{Ti}_2$
fw, g/mol	570.6
space group	$P2_1/c$
<i>a</i> , Å	15.276 (6)
<i>b</i> , Å	11.466 (3)
<i>c</i> , Å	20.151 (8)
β , deg	129.19 (3)
<i>V</i> , Å ³	2736
<i>Z</i>	4
<i>D</i> _{calcd} , g/cm ³	1.385
λ , Å	0.71069 (Mo K α)
μ , mm ⁻¹	6.83
maximum 2θ , deg	48
scan rate (deg/min ⁻¹)/max scan time (s)	1.7/40
total no. of reflections	5056
reflections used	4259
background time, s	3600
final no. of parameters	278
<i>R</i>	0.048
<i>R</i> _w	0.057

Table II. Refined Coordinates of $\text{C}_{32}\text{H}_{34}\text{Si}_2\text{Ti}_2$ ($\times 10^4$; Ti and Si, $\times 10^5$; H, $\times 10^3$) (*U*_{eq}, $\times 10^3$)

atom	<i>x</i>	<i>y</i>	<i>z</i>	<i>U</i> _{eq}
Ti(1)	18283 (7)	10194 (8)	79907 (5)	39
Ti(2)	33617 (7)	9583 (8)	70181 (5)	37
Si(1)	33246 (12)	23789 (12)	81613 (9)	43
Si(2)	16169 (11)	-1490 (12)	66240 (8)	40
C(11)	1994 (3)	-724 (4)	8711 (3)	67
C(12)	1879 (3)	218 (4)	9109 (3)	80
C(13)	2837 (3)	953 (4)	9494 (3)	81
C(14)	3543 (3)	465 (4)	9335 (3)	70
C(15)	3022 (3)	-571 (4)	8851 (3)	60
C(21)	5330 (3)	543 (3)	7960 (3)	61
C(22)	4888 (3)	85 (3)	8349 (3)	55
C(23)	4124 (3)	-826 (3)	7820 (3)	55
C(24)	4095 (3)	-930 (3)	7103 (3)	58
C(25)	4840 (3)	-84 (3)	7190 (3)	61
C(31)	652 (4)	2284 (4)	8072 (2)	69
C(32)	1051 (4)	2919 (4)	7705 (2)	77
C(33)	597 (4)	2396 (4)	6908 (2)	93
C(34)	-83 (4)	1437 (4)	6781 (2)	97
C(35)	-49 (4)	1368 (4)	7500 (2)	76
C(41)	1913 (3)	1246 (3)	5520 (2)	61
C(42)	2949 (3)	1129 (3)	5668 (2)	61
C(43)	3646 (3)	2091 (3)	6173 (2)	59
C(44)	3041 (3)	2802 (3)	6337 (2)	56
C(45)	1970 (3)	2280 (3)	5934 (2)	60
C(51)	4707 (3)	2859 (3)	9266 (2)	48
C(52)	5742 (3)	2831 (3)	9432 (2)	54
C(53)	6707 (3)	3276 (3)	10200 (2)	62
C(54)	6637 (3)	3749 (3)	10803 (2)	72
C(55)	5602 (3)	3778 (3)	10637 (2)	87
C(56)	4637 (3)	3333 (3)	9869 (2)	72
C(61)	1507 (3)	-1798 (3)	6378 (2)	45
C(62)	1310 (3)	-2081 (3)	5620 (2)	64
C(63)	1318 (3)	-3245 (3)	5423 (2)	73
C(64)	1523 (3)	-4126 (3)	5983 (2)	75
C(65)	1720 (3)	-3843 (3)	6740 (2)	82
C(66)	1712 (3)	-2679 (3)	6938 (2)	67
H(1)	286 (3)	350 (2)	771 (2)	50
H(2)	54 (2)	31 (4)	586 (2)	50
H(3)	394 (3)	208 (3)	778 (2)	50
H(4)	128 (3)	-10 (3)	722 (2)	50

spectrum to the structure shown in Figure 5.

Some Reactions of 2 and 3 and Related Compounds. Once **2** and **3** were isolated as pure compounds it was shown that not only did **2** transform spontaneously into **3** in solution but addition of PhSiH_3 to a solution of **3** regenerates **2**. Further, on standing for several days at room temperature, the solution NMR spectrum of **3** disappears and is replaced by broad resonances at very low

Table III. Some Selected Bond Lengths and Angles for $[\text{Cp}_2\text{TiSiH}_2\text{Ph}]_2$ (**2**)

Bond Lengths, ^a Å			
Ti(1)-H(4)	1.76 (3)	Ti(2)-Si(1)	2.851 (2)
Ti(1)-Si(1)	2.604 (2)	Ti(2)-Si(2)	2.583 (2)
Ti(1)-Si(2)	2.891 (2)	Ti(2)-H(3)	1.76 (3)
Ti(1)-Ti(2)	3.866 (2)	Si(1)-H(1)	1.47 (3)
Ti(1)-C(w)	2.057 (6)	Si(1)-H(3)	1.58 (3)
Ti(1)-C(y)	2.052 (4)	Si(1)-C(51)	1.943 (3)
Bond Angles, deg			
Si(1)-Ti(1)-H(4)	116 (1)	Ti(1)-H(4)-Si(2)	117 (2)
Ti(1)-Si(1)-H(3)	123 (1)	Ti(1)-Si(1)-H(1)	114 (2)
Ti(1)-Si(1)-C(51)	123.3 (1)	H(1)-Si(1)-C(51)	102 (2)
H(1)-Si(1)-H(3)	95 (2)	H(3)-Si(1)-C(51)	94 (1)
C(w)-Ti(1)-C(y)		130.5 (2)	

^aThe designators C(y) and C(w) refer to the Cp centroids in cis and trans relationships to the phenyl groups, respectively.

Table IV. Crystal Data and Parameters for Data Collection for $[\text{Cp}_2\text{Ti}]_2[\mu\text{-Si(H)(HPh)}](\mu\text{-H})$ (**3**)

formula	$\text{C}_{26}\text{H}_{28}\text{SiTi}_2$
fw, g/mol	464.4
space group	$P2_1/c$
<i>a</i> , Å	10.772 (3)
<i>b</i> , Å	11.129 (6)
<i>c</i> , Å	19.678 (8)
β , deg	112.94 (3)
<i>V</i> , Å ³	2172
<i>Z</i>	4
<i>D</i> _{calcd} , g/cm ³	1.420
λ , Å	0.71069 (Mo K α)
μ , mm ⁻¹	7.91
maximum 2θ , deg	45
scan rate (deg min ⁻¹)/max scan time (s)	1.7/40
tot no. of reflections	3507
reflections used	2303
background time, s	3600
final no. of parameters	230
<i>R</i>	0.046
<i>R</i> _w	0.062

field (δ 50 and 40) whose chemical shift temperature dependence verifies that they are due to paramagnetic species. This or these species also react with PhSiH_3 to regenerate **3** and subsequently **2**. Reaction of a solution of **3** with CO under ambient conditions leads in a few minutes to the formation of $\text{Cp}_2\text{Ti}(\text{CO})_2$ and PhSiH_3 in a mole ratio of 2:1. A similar reaction between **2** and CO leads to a much slower formation of $\text{Cp}_2\text{Ti}(\text{CO})_2$ (half-life several hours), a rate that corresponds to the rate of transformation of **2** to **3**.

Both the metastable titanocene, $[(\text{Cp}_2\text{Ti})_2]$, and the polymeric $[\text{Cp}_2\text{TiH}]_n$ reported by Bercaw and Brinzinger⁷ react rapidly with PhSiH_3 to give **2** and **3**, with evolution of H_2 and formation of polysilane.

Crystallographic Studies on Compounds 2 and 3. Crystal data and parameters for data collection for **2** are listed in Table I while atom coordinates and structural parameters are listed in Tables II and III, respectively. Figure 4 shows an Ortep drawing of one molecule of compound **2**. The molecule is a dimer of $\text{Cp}_2\text{TiSiH}_2\text{Ph}$, possessing C_2 symmetry, in which dimerization occurs via two Ti-H-Si bridges. The Si-H bridge bond is lengthened by about 0.1 Å relative to a terminal Si-H bond,⁸ indicating significant weakening of the bridging bond. However, the Ti-H bond length is about 0.2 Å shorter than that of the Ti-H-Ti bridge bond of **3** (see below). The six-membered ring composed of the Ti, Si, and bridging H atoms is only slightly

(7) Bercaw, J. E.; Marvich, R. H.; Bell, L. G.; Brinzinger, H. H. *J. Am. Chem. Soc.* **1972**, *94*, 1219.

(8) Allemand, J.; Gerdil, R. *Cryst. Struct. Commun.* **1979**, *8*, 927.

(9) Fieselmann, B. F.; Hendrickson, D. N.; Stucky, G. D. *Inorg. Chem.* **1978**, *17*, 2078. Francesconi, L. C.; Corbin, D. R.; Hendrickson, D. N.; Stucky, G. D. *Inorg. Chem.* **1979**, *18*, 3074. Francesconi, L. C.; Corbin, D. R.; Arrietta, W. C.; Hendrickson, D. N.; Stucky, G. D. *Inorg. Chem.* **1981**, *20*, 2059.

(6) Guggenberger, L. J.; Tebbe, F. N. *J. Am. Chem. Soc.* **1973**, *95*, 7870.

Table V. Refined Coordinates of $C_{26}H_{28}SiTi_2$ ($\times 10^4$; Ti and Si, $\times 10^5$; H, $\times 10^3$) (U_{eq} , $\times 10^3$)

atom	x	y	z	U_{eq}
Ti(1)	29670 (8)	38803 (7)	24718 (4)	20
Ti(2)	13088 (8)	37093 (7)	36626 (4)	22
Si(1)	3334 (22)	2312 (14)	3517 (11)	28
Si(2)	3234 (22)	2300 (14)	3628 (11)	28
C(11)	1387 (3)	2401 (3)	1800 (2)	29
C(12)	2638 (3)	2068 (3)	1772 (2)	30
C(13)	3003 (3)	2968 (3)	1373 (2)	34
C(14)	1977 (3)	3858 (3)	1154 (2)	36
C(15)	978 (3)	3508 (3)	1418 (2)	32
C(21)	1052 (3)	5335 (3)	4379 (2)	35
C(22)	1554 (3)	4349 (3)	4868 (2)	35
C(23)	2864 (3)	4071 (3)	4902 (2)	29
C(24)	3171 (3)	4886 (3)	4434 (2)	28
C(25)	2051 (3)	5667 (3)	4110 (2)	32
C(31)	4987 (3)	4755 (3)	3366 (1)	31
C(32)	5263 (3)	4388 (3)	2478 (1)	29
C(33)	4455 (3)	5091 (3)	2132 (1)	30
C(34)	3680 (3)	5893 (3)	2370 (1)	28
C(35)	4008 (3)	5685 (3)	3133 (1)	30
C(41)	-1103 (3)	3774 (3)	3029 (2)	38
C(42)	-619 (3)	2971 (3)	2628 (2)	31
C(43)	-28 (3)	1970 (3)	3089 (2)	33
C(44)	-146 (3)	2156 (3)	3775 (2)	39
C(45)	-810 (3)	3271 (3)	3738 (2)	39
C(51)	4930 (3)	1980 (3)	4422 (1)	28
C(52)	6188 (3)	2026 (3)	4376 (1)	30
C(53)	7333 (3)	1632 (3)	4967 (1)	34
C(54)	7219 (3)	1193 (3)	5604 (1)	35
C(55)	5961 (3)	1148 (3)	5651 (1)	36
C(56)	4816 (3)	1541 (3)	5060 (1)	32
H(1)	151 (3)	437 (4)	279 (2)	30
H(2)	235 (6)	262 (5)	390 (4)	30
H(3)	372 (5)	290 (6)	307 (3)	30
H(4)	285 (4)	109 (2)	327 (2)	30

Table VI. Some Selected Bond Lengths and Angles for $[Cp_2Ti]_2[\mu-HSi(HPh)]_2[\mu-H]$ (3)

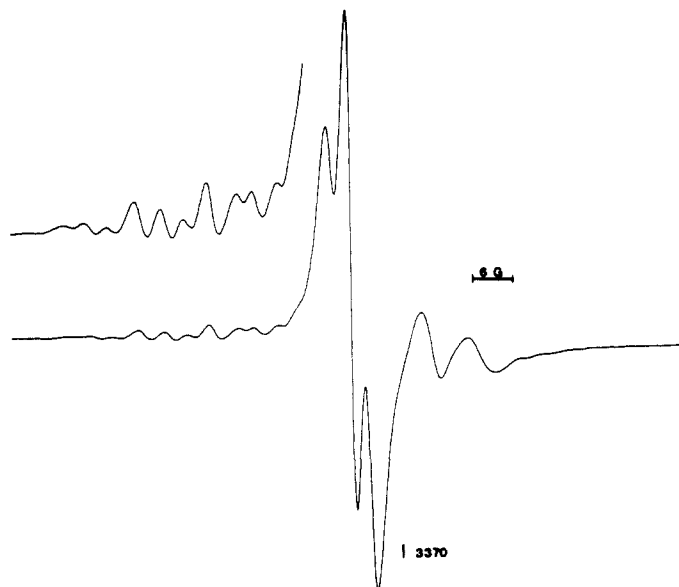
Bond Lengths, Å			
Ti(1)-Ti(2)	3.461 (1)	Ti(2)-H(1)	1.97 (3)
Ti(1)-H(1)	1.97 (4)	Ti(2)-Si(1)	2.78 (2)
Ti(1)-Si(1)	2.61 (2)	Ti(2)-H(2)	1.59 (6)
Si(1)-H(2)	1.56 (7)	Si(1)-H(4)	1.47 (3)
Si(1)-C(51)	1.97 (2)		
Bond Angles, ° deg			
H(1)-Ti(1)-Si(1)	80 (1)	H(1)-Ti(2)-H(2)	103 (3)
Ti(1)-Si(1)-H(2)	108 (3)	C(w)-Ti(1)-C(y)	130.6 (1)
C(x)-Ti(2)-C(z)	131.1 (1)	Ti(1)-H(1)-Ti(2)	124 (2)
Ti(1)-Si(1)-H(4)	116 (2)	Ti(1)-Si(1)-C(51)	130.5 (9)
H(4)-Si(1)-C(51)	101 (2)	H(2)-Si(1)-C(51)	97 (3)
H(2)-Si(1)-H(4)	98 (3)		

^aThe designators C(x) and C(y) refer to the Cp centroids that are cis, and C(w) and C(z) to those that are trans, to the phenyl group.

puckered. An unexpected feature of the structure is the cis disposition of the phenyl substituents on the silicon, relative to the plane of this ring. The NMR results had indicated the presence of only one isomer in solution, but we had expected this to be the trans isomer.

Crystal data and parameters for compound **3** are listed in Table IV while atom coordinates and structural parameters are listed in Tables V and VI, respectively. Figure 5 shows an Ortep drawing of the molecule. Compound **3** results from the extrusion of a SiHPh moiety from **2**. It has C_2 symmetry and crystallized as a racemate with two racemic pairs per unit cell. The extrusion of PhSiH leads to a reduction in the Ti-Ti (3.85 to 3.46 Å) and Ti-H (1.76 to 1.59 Å) distances, but the Ti-Si and Si-H distances remain unchanged.

ESR Spectra of 2 and 3. Compounds **2** and **3** both dissolve in toluene or tetrahydrofuran (THF) to give diamagnetic species as demonstrated by NMR spectroscopy. Toluene solutions of **2** give ESR spectra indicating the presence of several paramagnetic species at relatively low concentrations. The strongest signal

**Figure 6.** ESR spectrum of **2** in THF at ambient temperature.

broadens on lowering the temperature and only gives a broad featureless signal in the frozen glass. Its behavior in THF is quite different. Solutions prepared by prolonged agitation at -20°C gave an intense singlet ($g = 1.984$) with an overlapping, weaker singlet at slightly lower field. On warming the sample to room temperature, the spectrum rapidly changed to a sharp triplet ($g = 1.985$; $A(\text{Ti}) = 10.7$ G; $a(\text{H}) = 3.7$ G) due to a single electron coupling to a pair of equivalent protons and a second broad signal at $g = 1.984$. Apart from a sharpening of the signal, no changes were observed in this spectrum down to the freezing point of toluene. The room temperature spectrum is shown in Figure 6.

The ESR spectra of toluene solutions of **3** are shown in Figure 7. The spectrum at room temperature exhibits two signals, a broad featureless singlet at $g_{\text{iso}} = 1.984$ and the doublet of triplets characteristic of the mixed valence hydride **1**. On lowering the temperature and broad singlet becomes broader while the doublet of triplets intensifies in the manner expected for a species obeying the Curie law. The frozen solution spectrum is characteristic of the triplet state of a $Ti^{III}-Ti^{III}$ dimer⁹ ($g_{\parallel} = 1.9814$; $g_{\perp} = 1.9857$) superimposed on the spectrum of **1**. The triplet state assignment was confirmed by the observation of the forbidden transition at mid-field.

After standing for 2 days at room temperature all of the samples described above gave the spectrum of **1** as the principal signal.

Discussion

Compounds 2 and 3. To our knowledge only two compounds containing Ti-Si bonds have been fully characterized.¹⁰ In addition to being the first structurally characterized compounds containing a σ -bond between Ti(III) and an element of the carbon group, **2** and **3** have a number of other interesting features.

No compound containing an Si-H-X bridge (X = any element) has previously been reported. Given the propensity of aluminum to form such bridges, and given the proximity of Al and Si in the periodic table, the near total absence of such bridged compounds in the chemistry of silicon is surprising. The same disparity in behavior is of course encountered in the chemistries of boron and carbon and only recently have compounds with a C-H-M interaction (M = transition metal) been reported.¹² In a number of cases where such bonding might be expected, the carbon of an alkyl ligand prefers to bridge through a two-electron, three-center

(10) Rösch, L.; Altnau, G.; Erb, W.; Pickardt, J.; Bruncks, N. *J. Organomet. Chem.* **1980**, *197*, 51. Hencken, G.; Weiss, E. *Chem. Ber.* **1973**, *106*, 1747.

(11) Thompson, M. E.; Bercaw, J. E. *Pure Appl. Chem.* **1984**, *56*, 1. Green, M. L. H. *Pure Appl. Chem.* **1984**, *56*, 47. Brookhart, Green, M. L. H. *J. Organomet. Chem.* **1983**, *250*, 395.

(12) Holton, J.; Lappert, M. F.; Ballard, G. D. H.; Pearce, R.; Atwood, J. L.; Hunter, W. E. *J. Chem. Soc.* **1979**, 54.

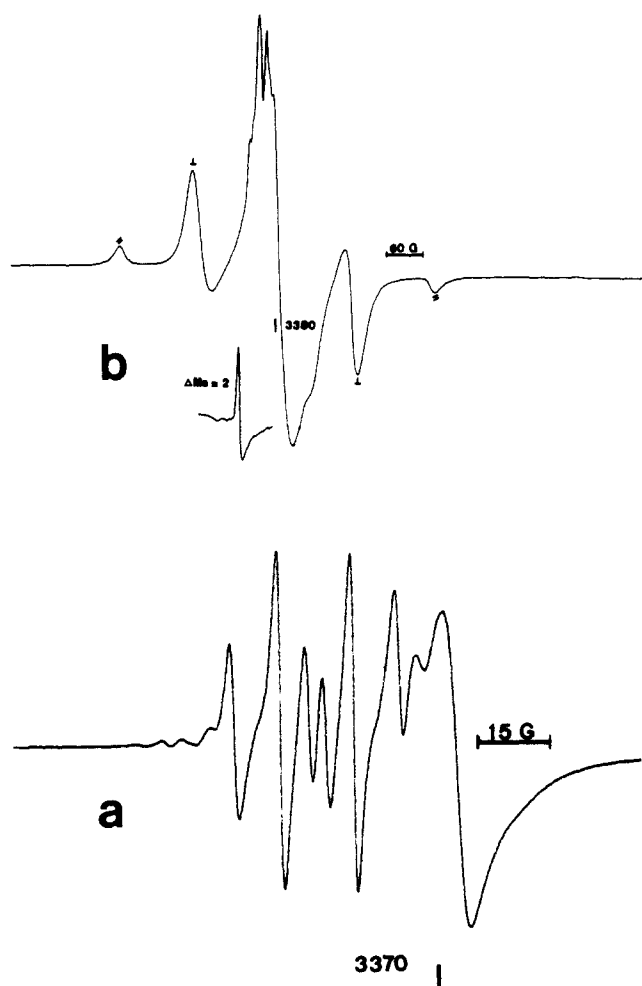
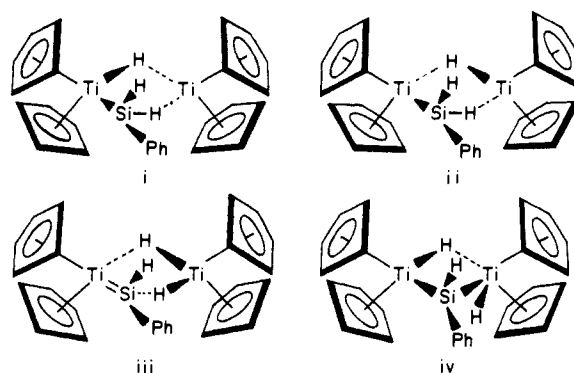


Figure 7. ESR spectrum of **3** in toluene (a) at ambient temperature and (b) at 170 K.

M–C–M bond.^{12,13} In the case of Si such bonding is probably precluded by the poor overlap of the $n = 3$ orbitals in such a three-center bond. The formation of the Si–H–Ti bond and the shortness of the Ti–H bond in this bridge relative to that in the Ti–H–Ti bridge of **3** reflect the electron and ligand deficiency of the Ti in the monomeric species.

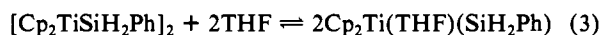
Following the NMR results, the only unexpected feature in the structure of **2** revealed by crystallography is the *cis* disposition of the two phenyl groups. There seems to be no obvious reason for this other than the demands of crystal packing forces. In solution, the NMR results indicate the presence of only a single isomer, but they do not distinguish between the two possibilities. The doubling of the hydride and Cp resonances on the *n*-hexyl- and benzylsilane reaction products indicate the presence of two isomers in those cases.

In the case of **2**, the constraints of reasonable valencies for the Ti and Si limit its description to being a silyltitanium(III) dimer. On the other hand, there is a structural ambivalence in the description of **3**, which is illustrated by structures i–iv. The shortness of the Ti–H bond bridging to silicon, relative to that bridging to Ti, is notable. A similar situation is evident in the aluminum compound reported by Guggenberger and Tebbe and referred to above.⁶ Since there is no evidence for encroachment of Cp hydrogens on the Ti–H–Ti bridge of the molecule, the longer bond cannot be attributed to steric effects. A more likely explanation for this effect is a substantial contribution of structure iv. In fact, the Ti–Si distance across the hydride bridge is only ca. 0.2 Å longer



than the direct Ti–Si bond, indicative of a significant covalent bonding interaction. In taking advantage of this interaction, the Ti is forced into a close approach to the H atom of the bridge. An alternative view of the same effect is that the Ti is coordinating to the σ -bonding electrons of the Si–H bond, thereby achieving a 16-electron count, as opposed to the 15-electron count available in structure ii. The constancy of the Ti–Si bond length in **2** and **3** and the proximity of the observed length to the sum of the covalent radii seem to favor structure ii, as does the observance of a triplet state in the ESR.

From the NMR evidence it is clear that both **2** and **3** substantially retain their dinuclear structures in solution. The temperature dependence of the NMR spectrum of **3** is unusual. Up to 80 °C none of the resonances show any sign of broadening again; on the contrary, they continue to broaden. We interpret this behavior as being due to the presence of the triplet state, rather than a dynamic process, and the depopulation of the triplet on cooling leads to sharpening of the spectrum. Such behavior has not been previously reported. Whereas **2** and **3** both exist predominantly as dinuclear, diamagnetic species in hydrocarbon solvents, in THF appreciable dissociation of **2** to a paramagnetic monomer occurs. The observation of a triplet (electron coupled to two equivalent protons) in the ESR spectrum of this monomer strongly supports its assignment as a THF-solvated phenylsilyltitanium(III) species produced by bridge-splitting of the dimer, thus



At –20 °C the reaction of **2** with THF is very slow (half-life > 1 h). At room temperature the reaction occurs almost as fast as dissolution, but it is still apparently slow enough on the NMR time scale that no paramagnetic effects are observed on the NMR spectrum of the dimer. Neither **1** nor **3** show any evidence in ESR spectra of dissociation in THF. The failure of **3** to show evidence of bridge splitting by THF may be a reflection of the tighter bonding of the Ti–H–Si bridge in this compound compared to **2**.

The ESR Spectra of 2 and 3. Given the relatively short Ti–Ti distance, the observation of a triplet state for **2** is rather surprising. The spin–spin interactions in $\text{Ti}^{\text{III}}\text{–Ti}^{\text{III}}$ dimer molecules have been extensively investigated by Stucky and co-workers.⁹ The zero-field splitting for **3**, derived from the spectrum shown in Figure 6, is 0.0509 cm^{-1} . Assuming that pseudodipolar coupling is negligible, the Ti–Ti distance (R) is calculated with eq 4,⁹ where D_{dd} is the

$$R = (0.650g^2/D_{\text{dd}})^{1/3} \quad (4)$$

zero field splitting due to dipole–dipole coupling. The value obtained, $R = 3.68 \text{ \AA}$, is in fair agreement with the value obtained from the crystal structure (3.46 Å), especially in view of the assumption about pseudodipolar coupling. Because of the relative scarcity of paramagnetic hydride complexes, very little is known about the properties of a bridging hydrogen atom in the transmission of superexchange effects. Most arguments suggest that it would be very effective, and a relatively strong antiferromagnetic interaction should result. A detailed study of the magnetic properties of this and related compounds is being undertaken to resolve this anomaly.

No triplet state was observed for **2**, a fact which also supports the idea that some special property of the Ti–H–Ti bridge is

(13) Huffman, J. C.; Streib, W. E. *J. Chem. Soc., Chem. Commun.* **1971**, 911.

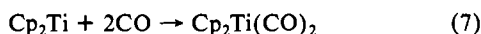
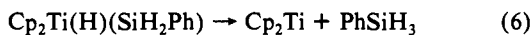
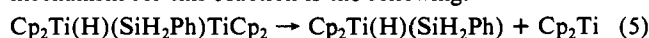
(14) Inensitive Nuclei Enhancement by Polarization Transfer. See: Morris, G. A.; Freedman, R. *J. Am. Chem. Soc.* **1979**, *101*, 760.

(15) Claus, K.; Bestian, K. *Justus Liebigs Ann. Chem.* **1962**, *654*, 8.

responsible for the appearance of the triplet state in **3**. The extended bridge through Si-H is less likely to transmit spin effects than the Ti-H-Ti bridge, and an antiferromagnetic coupling by direct overlap is probably operating in **2**.

Reactions of Compounds 2 and 3. The difference in behavior of **2** and **3** in THF is indicative of a significant difference in the strengths in their two bridging systems. Since we have observed the formation of $\text{Cp}_2\text{Ti}(\text{SiH}_2\text{Ph})$ from **2** in THF, and since the dissociation of $[\text{Cp}_2\text{TiH}]_2$ in THF to the paramagnetic Cp_2TiH has previously been observed by ESR by Bercaw and Brininger,⁷ the dissociation of **3** should be easily detected. The same is true for **1**, which also resists cleavage to mononuclear products in THF.

Toward CO, the reactivities of **2** and **3** are opposite to that observed with THF. At the very least, the evidence shows that **3** reacts much faster than **2**, and it is most likely that **2** only reacts by virtue of its decomposition to **3**. On the assumption that **3** gives the dicarbonyl via the liberation of free titanocene, a likely mechanism for this reaction is the following:

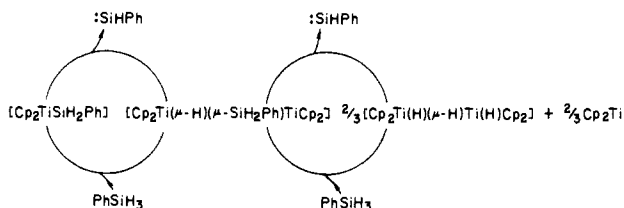


Such chemistry, if it is correct, supports the structural and spectroscopic evidence for a qualitative difference between the electron distributions in the bridging systems of **2** and **3**, with **2** having a propensity to cleave to two Ti(III) moieties in the presence of a σ -donor ligand and **3** disproportionating to a Ti(II), Ti(IV) pair in the presence of a strong π -acceptor.

The Mechanism of Silane Polymerization. As reported earlier,² there are no linear dimers or trimers detectable during the polymerization reaction. Polymer of the ultimate molecular weight is obtained even at low conversions of monomer, indicating that propagation occurs by a rapid addition reaction. The relatively low degree of polymerization but high turnover indicates the operation of a fairly rapid chain transfer process. Finally, the presence of SiH_2 end-groups was detected by application of a DEPT pulse sequence in the measurement of the ²⁹Si NMR spectrum of polymer sample.²

The above evidence strongly points to a mechanism involving chain growth at a metal coordination site. Involvement of free silyl radicals or of free silylene species would lead to the production of small chain or ring molecules which would be easily detected by NMR. On the other hand, no titanium species other than **1**, **2**, and **3** can be detected in actively polymerizing reaction mixtures, and the intensities of the spectra of these species in such reactions suggest that most of the titanium exists in this form.

It seems likely that propagation occurs by the repetitive insertion of a silylene moiety into a Ti-Si bond. The silylene moiety can be furnished by the transformation of **2** to **3** and of **3** to **1**, according to the following cycles.



How the silylene moieties become enchainned remains to be established.

Under a wide variety of reaction conditions, little variation has been observed in the degree of polymerization of the product polymer. Two likely candidates for a chain termination mechanism are hydrogenolysis of the Ti-SiHPh terminus to give an inactive SiH_2Ph chain end and a Ti-H species capable of reinitiating a new chain, or a homolytic scission of the Ti-Si bond followed by recombination of two silyl radicals. Either or both of these processes are plausible in view of the demonstrated conversion of both $[\text{Cp}_2\text{TiH}]_2$ and the metastable titanocene of Bercaw and Brininger to **1**, **2**, and **3** by phenylsilane. Although secondary silanes react readily with dimethyltitanocene to give blue/grey

reduced titanium products, they are not subject to catalytic dehydrogenative coupling. This great difference in the reactivity of primary and secondary silanes is the reason why the linear polymerization of primary silanes can occur.

We are presently studying the mechanism of the polymerization reaction in greater detail using kinetics and molecular weight studies.

Experimental Section

All manipulations were carried out under argon with standard inert atmosphere techniques. Toluene was freshly distilled from Na/benzophenone, and Fisher Scientific Co. anhydrous ether was used straight from the freshly opened can. Benzene-*d*₆ and toluene-*d*₈ were obtained from Merck Sharpe and Dohme, and THF-*d*₈ was obtained from Aldrich Chemical Co. All solvents were carefully purged by successive freeze-thaw cycles before use. Cp_2TiCl_2 was purchased from Alfa Ventron Corp. and used as received. $\text{Cp}_2\text{Ti}(\text{CH}_3)_2$ was prepared according to the published procedure,¹⁵ and after recrystallization it was stored in the mother liquor at -20°C in the dark. PhSiCl_3 was purchased from Petrarch Chemical Co. and used as received to prepare PhSiH_3 as described in the literature.¹⁶

Preparation of $[(\eta^5\text{-C}_5\text{H}_5)_2\text{Ti}(\text{HSiPhH})]_2$. PhSiH_3 (0.50 mL; 4.0 mM) was added to a solution of freshly recrystallized $\text{Cp}_2\text{Ti}(\text{CH}_3)_2$ (0.302 g; 1.45 mM) in toluene. The solution rapidly changed color from orange to blue/black with evolution of gas. Slow gas evolution continued for 24 h, after which time the supernatant liquid was decanted and the crystals were washed three times with 5-mL portions of cold diethyl ether. After the crystals were dried under vacuum the product was obtained as well-formed crystals (0.31 g; 75%) suitable for crystallography. Anal. Calcd for $\text{C}_{32}\text{H}_{34}\text{Si}_2\text{Ti}_2$: C, 67.35; H, 6.02; Si, 9.85. Found: C, 67.42; H, 6.10; Si, 9.77.

Preparation of $[(\eta^5\text{-C}_5\text{H}_5)_2\text{Ti}(\mu\text{-H})(\mu\text{-HSiPhH})]$. PhSiH_3 (0.15 mL; 1.2 mM) was added to a solution of $\text{Cp}_2\text{Ti}(\text{CH}_3)_2$ (0.247 g; 1.18 mM) in diethyl ether (3 mL). Within a few minutes a rapid color change from orange to blue/black occurred, accompanied by rapid gas evolution. After about 2 h, the supernatant liquid was decanted and the residual crystals were washed three times with 5-mL portions of cold diethyl ether and vacuum dried to give the pure product (0.165 g; 60%). Larger crystals for structure determination were obtained in lower yield by substituting 1:4 (v/v) toluene/ether for the ether reaction solvent in the above procedure. Anal. Calcd for $\text{C}_{26}\text{H}_{28}\text{Si}_2\text{Ti}_2$: C, 67.24; H, 6.09; Si, 6.05. Found: C, 67.08; H, 6.18; Si, 6.00.

Crystal Structure Determination. Crystal structures were determined at the Laboratoire des Structures aux Rayons-X, Université de Montréal. Samples were mounted under N_2 in a glass capillary. Measurements were made on an ENRAF-Nonius CAD-4 diffractometer. The unit cell was determined from a set of 25 reflections collected with the SEARCH procedure. The space group was determined by oscillation photographs and subsequently confirmed by systematic absences in the complete data set ($h0l, l \neq 2n$ and $0k0, k \neq 2n$) to be $P2_1/c$. Intensity data were collected with use of the $\omega/2\theta$ technique with a fixed slit width of 4.0 mm and a scan range of $\omega = (1.00 + 0.35 \tan \theta)^\circ$, extended 25% on each side for background. Collection was at room temperature for **2**. Five standards were measured per hour, and a variation of less than 2% was observed in their intensities. Data for **3** were collected at low temperature, due to extensive decomposition in crystals irradiated at room temperature. The intensities of a set of seven standards decreased by less than 5% during the data collection at low temperature. Data were corrected for Lorenz and polarization effects but, because of the low absorption coefficients, were not corrected for absorption.

In both structures, the Cp and phenyl groups were refined as ideal polygons (C-C 1.420 Å for Cp and C-C 1.395 Å for phenyl). For **2**, isotropic refinement of all non-hydrogen atoms and anisotropic refinement of Si and Ti converged to $R = 0.091$. Anisotropic refinement of all non-hydrogen atoms converged to $R = 0.062$. The hydrogen atoms of Cp and phenyl groups were positioned by using their ideal coordinates ($U = 0.01 \text{ \AA}^2$). Hydrogen atoms attached to silicon were located on a ΔF map and refined by using constrained distances ($U = 0.05 \text{ \AA}^2$). In the final cycles, individual weights $w = 1/\sigma^2(F)$ based on counting statistics were applied. The general background in the final ΔF map was lower than $\pm 0.4 \text{ e/\AA}^3$. When the same procedure was used compound **3** refined to an R value of 0.061 for a six-membered ring (Ti_2SiH_3), but with a large anisotropy on the silicon atom. A disordered silicon was introduced into the model, and the two occupancy factors were refined. The final positions for the two Si atoms showed equal occupancy at a separation of 0.3 Å, and this refinement converged to $R = 0.046$. The

(16) Benkeser, R. A.; Landesman, H.; Foster, D. J. *J. Am. Chem. Soc.* 1952, 74, 648.

final ΔF map had a background of $\pm 0.5 \text{ e}/\text{\AA}^3$.

The scattering curves were taken from Cromer and Waber¹⁷ except for that of hydrogen, which was from Stewart et al.¹⁸

NMR and ESR Spectra. Proton spectra were measured on a Varian XL-200 FT spectrometer. The inept spectrum shown in Figure 3 was measured on a Varian XL-300 FT machine at 59.59 MHz. The sample was a saturated solution in THF at -80°C and was referenced to external Me_4Si in CDCl_3 (1:1 (v/v)) at ambient temperature. The following pulse sequence was used for the proton-decoupled spectrum: $90^\circ(\text{H}, x) - \tau/2 - 180^\circ(\text{H}, x)$, $180^\circ(\text{Si}, x) - \tau/2 - 90^\circ(\text{H}, y)$, $90^\circ(\text{Si}, x) - \Delta/2 - 180^\circ(\text{H}, x)$, $180^\circ(\text{Si}, x) - \Delta/2$ -decouple-acquire.

For both coupled and decoupled spectra the following parameters were used: $\text{PW}(90^\circ)_\text{H} = 41.1 \mu\text{s}$, $\text{PW}(90^\circ)_\text{Si} = 21.5 \mu\text{s}$. The FIDs were collected into 32 K data points. Since no silicon satellites were observed in the ^1H spectrum, a J value of 200 Hz was initially used, based on the reported value for PhSiH_3 .¹⁹ A spectral width of 50 KHz was employed with a digital resolution of 3.3 Hz. A refocussing delay of 1.67 ms was used in conjunction with an excitation delay of 2.5 ms and an equilibrium delay of 2 s. A coupled spectrum was subsequently run with use of the

(17) Cromer, D. T.; Waber, J. T. *Acta Crystallogr.* **1965**, *18*, 104.

(18) Stewart, R. F.; Davidson, E. R.; Simpson, W. T. *J. Chem. Phys.* **1965**, *42*, 3175.

(19) Jensen, M. A. *J. Organomet. Chem.* **1968**, *11*, 423.

same conditions to obtain a more accurate $J_{\text{Si-H}}$ value, and the parameters were then modified to optimize the coupled spectrum. The modified parameters were $J_{\text{Si-H}} = 150 \text{ Hz}$, spectral width = 7142.9 Hz, digital resolution = 0.45 Hz, excitation transfer delay = 3.33 ms, and equilibrium delay = 1 s.

Acknowledgment. This work was supported by grants from the Natural Sciences and Engineering Research Council of Canada, the Fonds FCAC de Québec, and the Dow Corning Corp. Two of us (J.F.H. and E.S.) thank the Governments of France and Québec for travel grants in support of this project. Valuable discussions with Dr. D. Gourier, Laboratoire de la chimie de la matière condensée, ENSCP, on the subject of ESR spectra, and with Dr. M. Simard, Laboratoire des structures aux rayons-X, concerning the crystal structures, are gratefully acknowledged.

Supplementary Material Available: Calculated positions for hydrogen atoms of phenyl groups and Cp rings for **2** (Table VII) and **3** (Table VIII), anisotropic thermal parameters for non-hydrogen atoms of **2** (Table IX) and **3** (Table X), and calculated and observed structure factor amplitudes for **2** (Table XI) and **3** (Table XII) (6 pages). Ordering information is given on any current masthead page.

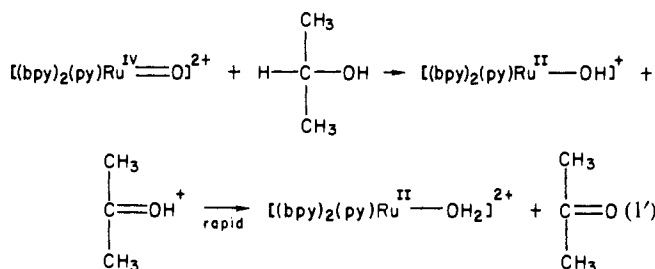
Hydride Transfer in the Oxidation of Formate Ion by $[(\text{bpy})_2(\text{py})\text{Ru}(\text{O})]^{2+}$

Lee Roecker and Thomas J. Meyer*

Contribution from the Department of Chemistry, The University of North Carolina, Chapel Hill, North Carolina 27514. Received October 1, 1985

Abstract: The kinetics of oxidation of formic acid/formate ion by $[(\text{bpy})_2(\text{py})\text{Ru}^{\text{IV}}(\text{O})]^{2+}$ (bpy is 2,2'-bipyridine and py is pyridine) have been studied as a function of pH and temperature, and the kinetics of oxidation of HCO_2^- by $[(\text{bpy})_2(\text{py})\text{Ru}^{\text{III}}(\text{OH})]^{2+}$ have been studied at pH 7. The pH dependence of the Ru^{IV} reaction is consistent with paths involving oxidation of HCO_2H , k (25 $^\circ\text{C}$, $\mu = 0.1 \text{ M}$) = $0.01 \pm 0.04 \text{ M}^{-1} \text{ s}^{-1}$, and of HCO_2^- , k (25 $^\circ\text{C}$, $\mu = 0.1 \text{ M}$) = $4.2 \pm 0.2 \text{ M}^{-1} \text{ s}^{-1}$. For the oxidation of HCO_2^- by Ru^{III} , k (25 $^\circ\text{C}$, $\mu = 1.0 \text{ M}$, pH 7) = $0.01 \text{ M}^{-1} \text{ s}^{-1}$. The path involving Ru^{IV} and HCO_2^- exhibits a large kinetic isotope effect with $k_{\text{HCO}_2^-}/k_{\text{DCO}_2^-} = 19$ (25 $^\circ\text{C}$, $\mu = 1.0 \text{ M}$) while that involving Ru^{III} and HCO_2^- has a much smaller kinetic isotope effect with $k_{\text{HCO}_2^-}/k_{\text{DCO}_2^-} = 3$ (25 $^\circ\text{C}$, $\mu = 1.0 \text{ M}$). Spectral evidence, in conjunction with the isotope effect data, suggests that oxidation of HCO_2^- by $[(\text{bpy})_2(\text{py})\text{Ru}^{\text{IV}}(\text{O})]^{2+}$ occurs by a two-electron, hydride transfer which is discussed in some detail. Oxidation of HCO_2^- by $[(\text{bpy})_2(\text{py})\text{Ru}^{\text{III}}(\text{OH})]^{2+}$ appears to occur by outer-sphere electron transfer.

An important theme in our recent work has been the preparation and characterization of polypyridyl oxo complexes of ruthenium-(IV)^{1,2} and an examination of their abilities as stoichiometric and catalytic oxidants.^{3,4} The results of mechanistic studies suggest that oxidation of 2-propanol to acetone⁵ and of cumene to cumyl alcohol⁶ proceed by two-electron, hydride transfers, e.g., reaction 1', oxidation of hydrogen peroxide to oxygen via hydrogen atom transfer,⁷ and oxidation of PPh_3 to OPPh_3 by O-atom transfer.⁸ One of the notable features about the polypyridyl complexes as



(1) (a) Moyer, B. A.; Meyer, T. J. *Inorg. Chem.* **1981**, *20*, 436. (b) Dobson, J., work in progress.

(2) Takeuchi, K. J.; Thompson, M. S.; Pipes, D. W.; Meyer, T. J. *Inorg. Chem.* **1984**, *23*, 1845.

(3) (a) Thompson, M. S.; DeGiovanni, W. F.; Moyer, B. A.; Meyer, T. J. *J. Org. Chem.* **1984**, *49*, 4972. (b) Moyer, B. A.; Thompson, M. S.; Meyer, T. J. *J. Am. Chem. Soc.* **1980**, *102*, 2310.

(4) Meyer, T. J. *J. Electrochem. Soc.* **1984**, *131*, 221C.

(5) (a) Thompson, M. S.; Meyer, T. J. *J. Am. Chem. Soc.* **1982**, *104*, 4106.

(b) Roecker, L.; Meyer, T. J., submitted for publication.

(6) Thompson, M. S.; Meyer, T. J. *J. Am. Chem. Soc.* **1982**, *104*, 5070.

(7) (a) Gilbert, J. A.; Gersten, S. W.; Meyer, T. J. *J. Am. Chem. Soc.* **1982**, *104*, 6872. (b) Gilbert, J. A.; Roecker, L.; Meyer, T. J., manuscript in preparation.

(8) Moyer, B. A.; Sipe, B. K.; Meyer, T. J. *Inorg. Chem.* **1981**, *20*, 1475.

oxidants is that they are easily amenable to kinetic studies and detailed mechanistic investigations based on ^{18}O labeling, pH dependence, H/D kinetic isotope effects, and initial product studies the latter of which can sometimes allow a distinction to be drawn between one- and two-electron pathways.

We report here a detailed study on the oxidation of formate ion and formic acid by $[(\text{bpy})_2(\text{py})\text{Ru}(\text{O})]^{2+}$ to give CO_2 . In addition to a general interest in C-based redox chemistry, two points drew our attention to the formate/formic acid reaction. The first is that the oxidation of formate by a variety of oxidants has been reported which allows for comparisons to be made between their reactivity characteristics and those of oxo complexes